ARTICLE

Check for updates

Evolution of eastern Tibetan river systems is driven by the indentation of India

Yi Chen[1], Baosheng Wu [1✉], Zhongyu Xiong[2], Jinbo Zan[2], Bangwen Zhang[1], Ruoyin Zhang[1], Yuan Xue[1], Minhui Li[1] & Bingshuai Li[3]

The main rivers that originate from the Tibetan Plateau are important as a resource and for the sedimentary and biogeochemical exchange between mountains and oceans. However, the dominant mechanism for the evolution of eastern Tibetan river systems remains ambiguous. Here we conduct geomorphological analyses of river systems and assess catchment-average erosion rates in the eastern Tibetan Plateau using a digital elevation model and cosmogenic radionuclide data. We find that major dividing ranges have northeast oriented asymmetric geometries and that erosion rates reduce in the same direction. This coincides with the northeastward indentation of India and we suggest this indicates a primarily tectonic influence on the large-scale configuration of eastern Tibetan river systems. In contrast, low-level streams appear to be controlled by fluvial self-organization processes. We propose that this distinction between high- and low-order channel evolution highlights the importance of local optimization of optimal channel network models in tectonically active areas.

[1] State Key Laboratory of Hydroscience and Engineering, Department of Hydraulic Engineering, Tsinghua University, Beijing 100084, China. [2] Key Laboratory of Continental Collision and Plateau Uplift, Institute of Tibetan Plateau Research, and Center for Excellence in Tibetan Plateau Earth Sciences, Chinese Academy of Sciences, Beijing 100101, China. [3] School of Earth Sciences, East China University of Technology, Nanchang 330013, China. ✉email: baosheng@tsinghua.edu.cn

The evolution of river systems and associated ecosystems represents fundamental, yet poorly understood, problems in the multidisciplinary earth sciences[1]. Conventional river systems analyses, including dividing range and drainage network interpretation, build on the assumption that dividing ranges are relatively static[2,3]. Recent studies have suggested that divides are more mobile than previously thought and that divide mobility activates feedbacks on the landscape, such as the establishment of new drainage networks[1,4], the hanging of flat surfaces in craggy mountain ranges[5], landslide diversion[6], and headward migration of the knickpoint[7]. Those discoveries imply an imperfect understanding of the dynamical interactions among tectonic, climatic, and fluvial processes.

The growth of the Tibetan Plateau is one of the most important geological events in the Cenozoic (Fig. 1). And the collision and continued convergence between Indian and Eurasian plates have created substantial tectonic deformation over the Tibetan Plateau[8]. The development of the Tibetan Plateau has been proposed to account for the configuration of Asian river systems (Fig. 1)[5,9–13], and a fundamental question about the evolution of the Tibetan orogenic system is the relationships among deformation, precipitation, and erosion[14]. To decipher the connection between tectonic and fluvial processes in the eastern Tibetan Plateau, Zeitler et al.[15] proposed positive feedback existed between tectonic-fluvial interaction in the eastern Himalayan syntaxis. Korup and Montgomery[16] recognized glacial damming of the Yarlung River, which could preserve the drainage networks and plateau edge. Wang et al.[17] suggested that the rapid uplift was the controlling factor for the organization of drainage networks and steepening of the Yarlung Gorge. Zhang et al.[18] presented that the isostatic crust rebound in the northeastern Tibetan Plateau drove drainage reorganization. These studies are focused on the longitudinal profiles and vertical incisions of eastern Tibetan rivers, while studies on the regional geometry of river systems have been scarce[9,19]. The regional structure of the river system contains extensive information corresponding to tectonic and climatic influences[20]. Morphological analysis of river systems can be used to reveal the development of the river system and provide insight into the evolution of landscape[1,3].

Here, we present a quantitative morphological analysis of the dividing ranges and drainage networks in the eastern Tibetan Plateau, combined with evidence from catchment-average erosion rates, to explore the evolution of eastern Tibetan river systems. Our study, focusing on a rich interdisciplinary problem in earth science, reveals the coevolution and dynamical links between river systems and tectonic plates in the eastern Tibetan Plateau, investigates the relative contribution of exogenic tectonic process and endogenic self-organization at different levels of river system evolution and sheds insight on the development mechanism of Tibetan orogenic system.

Results and discussion

Morphological characteristics of river systems. Our analysis of the eastern Tibetan Plateau river systems contains two components: the dividing ranges and the drainage networks (Fig. 2). Given the truncated catchment boundaries in the eastern Tibetan Plateau, the Gilbert metrics including the across-divide difference in hillslope relief and divide asymmetry index (see Methods), are accounted for in our study of the structures of dividing ranges[21]. Gradient works well in some regions, but there are challenges associated with the development of threshold slopes in the high-relief part of the eastern Tibetan Plateau[22]. The Gilbert metrics are computed using the TopoToolbox v2 topographic analysis software[23] to quantitatively identify asymmetric dividing ranges (see Methods, and Supplementary Data 1).

The southernmost asymmetric dividing ranges are identified along the northern boundaries of the Parlung River catchment (Fig. 2), with eastern Himalayan syntaxis as the core, the vectors of divide asymmetry spread outwards in a radial pattern. Rectangular tributary junctions are observed throughout the peculiar eastern Himalayan syntaxis river networks (Supplementary Fig. 1a). The Parlung River drops by approximately 2 km from headwater to its confluence with the Yarlung River, a remarkable knickpoint is found in the profile of Parlung River at an elevation of 2700 m (Supplementary Fig. 1b). Both the rectangular tributary junctions and knickpoint mark the capture of the Parlung River by the Yarlung River[24], and the northern movement of dividing ranges.
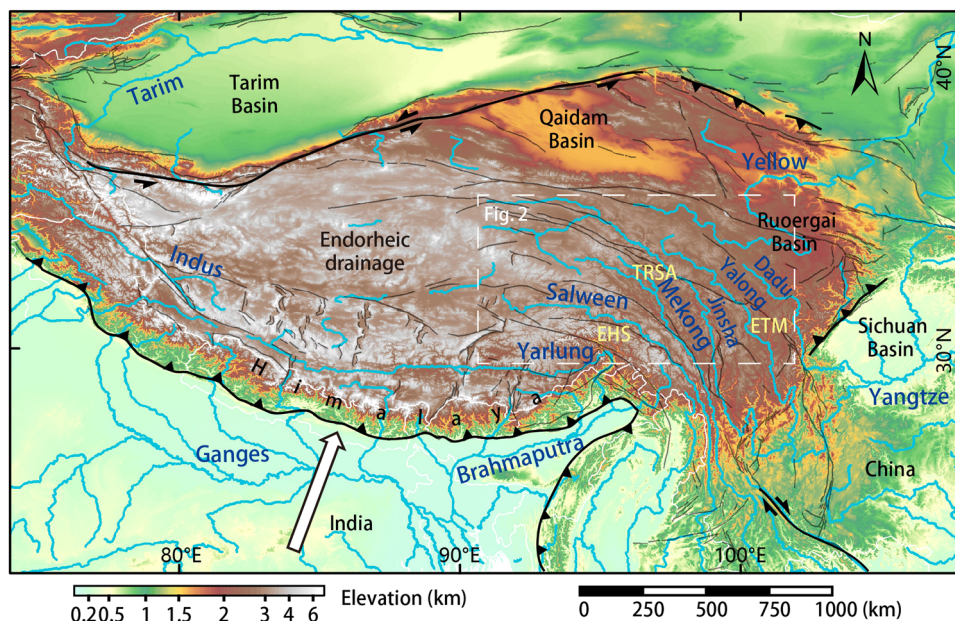

Fig. 1 Topography, major Asian rivers, and principal faults of the Tibetan Plateau. Major Asian rivers are shown as cyan lines, principal faults are displayed as black lines. The dotted write square denotes the location of Fig. 2. Write arrow indicates the northeastward indentation of India. Abbreviations: EHS = eastern Himalayan syntaxis, TRSA = Three Rivers Source Areas, ETM = eastern Tibetan Plateau margin.
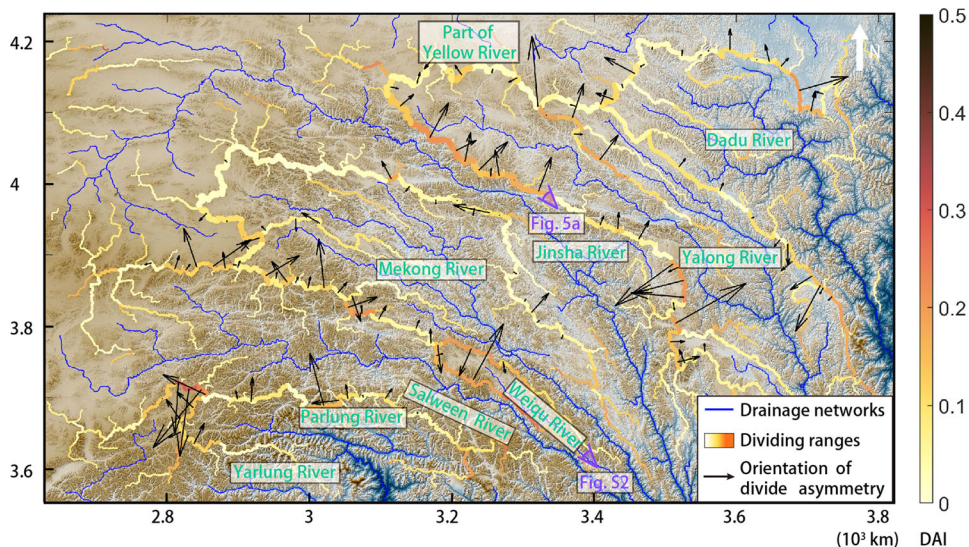
Fig. 2 Macroscopic configuration of the river systems in the eastern Tibetan Plateau. High-order drainage networks (stream-order ≥ 7) are shown as blue lines. High-level dividing ranges (divide distance $\geq 5 \times 10^5$ m) are colored by the values of divide asymmetry index (DAI), with line thickness denoting divide distance. Black arrows indicate the orientations of divide asymmetry and lengths scaled by the magnitudes of divide asymmetry. Map projection is Universal Transverse Mercator (UTM, WGS 1984, zone 42 N).

It is apparent that asymmetric dividing ranges are widely distributed within the central part of the eastern Tibetan Plateau named Three Rivers Source Areas. These noteworthy asymmetrical dividing ranges are situated at the boundaries of the Salween and Mekong rivers, and the Jinsha and Yalong rivers (Fig. 2). The regional orientations of divide asymmetry are mainly northeast, while some segments show smaller asymmetry trends to the opposing southwestern direction. The Weiqu River, located between the trunks of the Salween and Mekong rivers, shows inward asymmetric characteristics (Fig. 2). The concomitance of low-relief surface in the Weiqu catchment and distinctly inward escarpments along the asymmetrical eastern and western dividing ranges (Supplementary Fig. 2) suggests loss of catchment area to its larger neighbors.

Another noteworthy asymmetric dividing range are located at the eastern Tibetan Plateau margin. The asymmetries tend toward the interior of the Yellow River catchment (Fig. 2). In the southern part of Ruoergai Basin (Fig. 1), the streams of Yellow River show tributary junctions at a rectangular angle, and parallel with the directions of divide asymmetry at the boundaries between Yellow and Dadu catchments, this fluvial structure may reflect geometric control by exogenic drivers.

The quantitative Gilbert metrics give us the opportunity to evaluate the discrepancy between low-level divide segments (divide distances $< 5 \times 10^5$ m) and higher-level segments (divide distances $\geq 5 \times 10^5$ m) (Fig. 3a). The directions of asymmetry along low-level divide segments correspond to the northeast, southwest, and west azimuths of catchment boundaries, and have no preferential direction. The high-level dividing ranges are concentrated in the unique northeast orientation, the 95% confidence intervals of asymmetric directions are 340.14°–26.64° (see Methods).

The structural properties of eastern Tibetan drainage networks are expressed as the area ratios (R_a) and length ratios (R_l) in different Horton–Strahler orders (Supplementary Data 2). R_a is calculated as the ratio of the average area of streams of order i (A_i) to the average area of streams of order $i-1$ (A_{i-1}), and R_l is calculated in a similar manner (see Methods). The values of R_a and R_l are around 4.6 and 2.1 for low-order streams, respectively. Convergences occur at stream-orders of 1–5; and deviate begins as the stream-order increases (Fig. 3b, c). For low-order
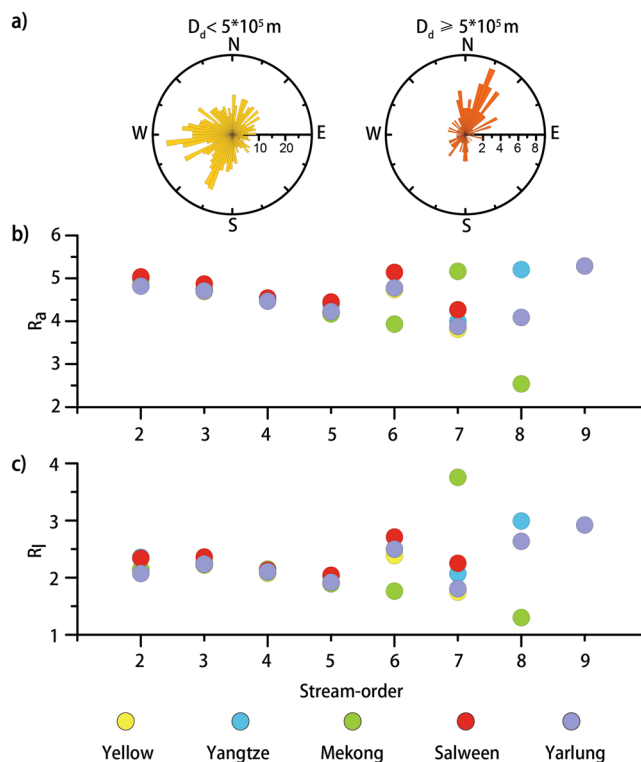

Fig. 3 Morphological characteristics of the eastern Tibetan dividing ranges and drainage networks. a Directions of the divide asymmetry sectioned by divide distance (D_d). **b** Area ratios (R_a) of the five continental rivers. **c** Length ratios (R_l) of the five continental rivers.

(1–5) streams, the values of R_a and R_l are approximately invariant, both conform to the scale-invariant Horton's Law of drainage networks, which is tied to the establishment of a dynamically suboptimal state[25,26].

The low and high levels' diverse characteristics of dividing ranges and drainage networks imply the interacting roles of
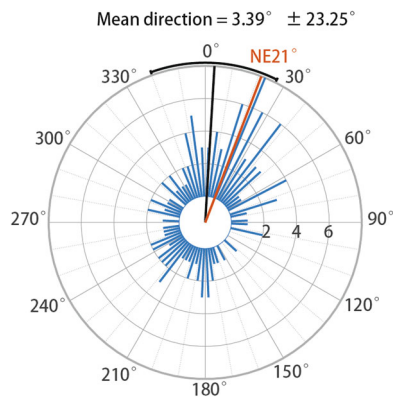
Mean direction = 3.39° ± 23.25°

Fig. 4 Directional statistics of the directions of asymmetry along the high-level divide. Black lines denote the mean and the upper and lower 95% confidence limits on the mean of the directions. The orange line indicates the direction of the persistent indentation of India. The population of the directions of asymmetry along the high-level divide is shown in the blue histograms.

endogenic and exogenic processes. The topological self-similarity in low-order streams integrated the characteristic that low-level divide segments have no preferential orientation (Fig. 3), suggest that low-level river systems are dominated by endogenic in-stream processes. The gradual divergences of the R_a and R_l with increasing stream-orders and the prevalent northeast asymmetric directions of the major dividing ranges (Fig. 3) reflect the relative dominance of exogenic drivers, such as tectonic or climatic perturbations.

Evidence of river systems evolution. The morphological characteristics of the river system lack explicit time information, which may be insufficient to illuminate dynamic processes. River system evolution can also be inspected through the spatial variations of erosion rates[27]. Catchment with higher erosion rate grows at the expense of adjacent catchment featuring lower erosion rate, the across-divide difference in erosion rates can cause the development of river networks[28]. The average erosion rate of the catchment (E_{cat}) quantifies the coupling of hillslope and fluvial processes, which is effective in uncovering the divide mobility[6]. We focus on the available cosmogenic radionuclide catchment erosion rates of the eastern Tibetan Plateau from the OCTOPUS database (an open cosmogenic isotope and luminescence database, see details in Methods)[29].

The E_{cat} values of eastern Himalayan syntaxis range from 0.1 to 4 mm/y[30], extremely high values coincide with the locus of longer-term incision rates by thermochronologic studies[31]. The radial pattern of the divide asymmetry is well defined by the periphery of the bull's eye-like rapid exhumation region. Finnegan et al.[30] found that the spatial comparisons between exhumation rates and mean topographic reliefs reveal a correspondence of exhumation rates and topographic reliefs. There is no clear relationship between precipitation patterns and exhumation rates within the eastern Himalayan syntaxis. The concurrence between morphological features (Fig. 2) and dynamic erosion processes suggests that the northward migrations of divides are driven by the ongoing northward advance of the eastern Himalayan syntaxis[31].

The peak E_{cat} values are 8 and 0.5 mm/y for the main streams of the Salween and Mekong rivers, respectively[32]. One-order decrease in erosion rates is parallel to the northeast directions of divide asymmetry at the boundaries between Salween and Mekong rivers (Fig. 2). Multiple regressions suggest that erosion rates in the Salween and Mekong River catchments are better

explained by mean local relief than mean annual precipitation[32]. The drainage area loss of the Weiqu River is verified by the lower E_{cat} of the Weiqu River (<0.1 mm/y)[32] relative to the adjacent Salween and Mekong rivers. The downstream compact juxtaposition of the Salween, Mekong, and Yangtze rivers records the substantial crustal strains caused by the convergence between Indian and Eurasian plates[19], the upstream divides migration would seem to support this inference.

The E_{cat} values span an order of magnitude from 0.03 to 0.6 mm/y in the eastern Tibetan Plateau margin. In the Yellow River catchment (Fig. 2), the E_{cat} values are ~0.06 mm/y[33,34], which are smaller than those from the southern Yangtze River watershed (0.2–0.6 mm/y)[33,35]. Combined with the orientations of divide asymmetry, this pattern would imply divide migrations to the interior of Yellow River catchment, which means that the drainage area acquisition of the Yangtze River was gained from the Yellow River. Ansberque et al.[33] proposed that the relationships between erosion rates versus mean annual precipitations do not display any clear correlations within the eastern Tibetan Plateau margin. And indeed, there is a nonlinear relationship between erosion rates and normalized channel steepness indexes[35].

The above analyses suggest that differences of Gilbert metrics across divides can successfully indicate divide movement by catchment erosion and snapshot the transient processes in river systems. The existences of rectangular tributary junctions, knickpoint in longitudinal profile (Supplementary Fig. 1), low-relief surface, and distinctly escarpments along asymmetric dividing ranges (Supplementary Fig. 2) are further evidence of former or ongoing motion of divides, such geomorphic features map the hotspots of the dynamic fluvial landscape.

The controlling factors of eastern Tibetan river systems evolution. From these observations in the eastern Tibetan Plateau, an issue was raised: which factor is the dominant force driving river systems evolution, i.e., exogenic tectonic or climatic drivers[2] or endogenic self-organization by minimizing the energy expenditure of open dissipative system[36]. Since climatic drivers usually shape landscape through erosion and sedimentation by the flow of water, we use the mean annual precipitation (MAP) as an indicator of climatic drivers (see Methods). MAP rates vary from 176 to 1746 mm/y across the eastern Tibetan Plateau (Supplementary Fig. 3). High values are observed in parts of the major river valleys (Yurlung and Salween rivers), which serve as the moisture paths of the South Asian Monsoon. Except for the valley regions, a westward decrease of MAP amounts is observed from the windward side to the leeward side of the eastern Tibetan Plateau, and a directionally dependent pattern of northeastward-decreasing MAP amounts is not borne out in our study area. There is no correlation between the spatial variations of precipitation and the northeastern orientations of divide migration. Instead, both the Three Rivers Source Areas and the eastern Tibetan Plateau margin catchments with conspicuous asymmetric dividing ranges and variations in E_{cat} are located in regions with similar amounts of precipitation. Our results are consistent with the previous studies[14,30,32,33,37] and suggest that rainfalls have a limited impact on the denudation and evolution of river systems across the eastern Tibetan Plateau.

Here, we propose that the macroscopic configuration of eastern Tibetan river systems is controlled by the parallel tectonic stress caused by the movement of the Indian plate. Directional statistics (see Methods) suggests that the direction of persistent convergence between the India and Eurasia plates (NE 21°)[38,39] coincides with the main orientations of high-level divide migration (Fig. 4). The collision and continued convergence
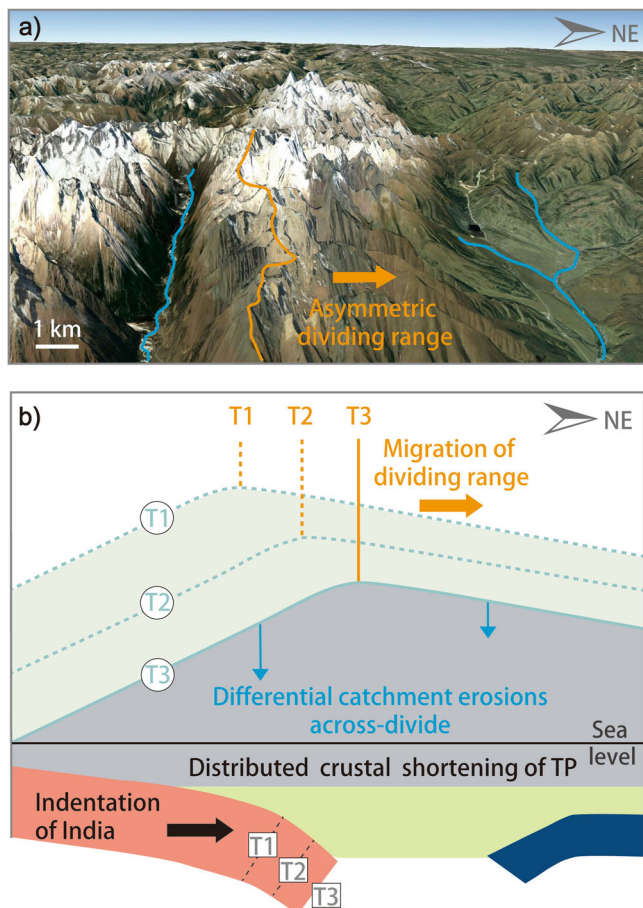
Fig. 5 Simplified model to illustrate the dynamical links between river systems and tectonic plates in the eastern Tibetan Plateau (TP). a A dividing segment between the Jinsha and Yalong catchments, oblique view toward the northwest of satellite image draped on digital elevation model (3×vertical exaggeration, from Google Earth), seen from the perspective point indicated on Fig. 2. The orange line indicates the dividing range, blue lines denote the river networks. The asymmetric dividing range will migrate farther northeast (NE) according to the divide asymmetry index. **b** Above the sea level line, the conceptive representation of the evolution of eastern Tibetan river systems, modified after Forte and Whipple[21]. The dividing range moves when catchment erosion rates are different across-divide. Orange arrow indicates the northeastward migration of the dividing range. Under the sea-level line, a cross-section of convergent plates in the eastern Tibetan Plateau. The black arrow shows the persistent northeastward indentation of India. The crust is displayed grayish and not distinguished between India and Eurasia. Indian mantle lithosphere is marked red. Eurasian mantle lithosphere is marked blue, green area represents the crushed lithospheric region.

between Indian and Eurasian plates have caused India to penetrate ~2000 km into Eurasia[8,40]. Substantial crustal shortening accommodates much of India's 36-40 mm/y of convergence with Eurasia[38,41]. Modern Tibetan topography is primarily created by the indentation of Indian plate[8]. In the southwestern sides of eastern Tibetan asymmetric divides, which are characterized by a relatively higher hillslope relief, catchment erosions are faster than those in the northeastern sides with a low hillslope relief (Fig. 5). Spatial variations in hillslope reliefs and erosion rates give rise to the northeastward migration of river systems, the river systems coevolve toward the configuration which would equalize the topographic asymmetries and tectonic strain. The robust relationship between the orientations of high-level divide

migration and strain field suggests that the persistent northeastern indentation of India powers the evolution of eastern Tibetan river systems.

Numerical modeling studies suggested that lateral advection can impact drainage divide location and landscape evolution[42–45]. When there is a trend of velocity gradient across the Tibetan Plateau in the direction of NE 21° (Supplementary Fig. 4)[38,46,47], we infer that the distributed shortening in the eastern Tibetan Plateau is a sufficient condition to cause rock moves towards the northeast with respect to the Earth's surface. The northeast advection in the eastern Tibetan Plateau could push the high-level drainage divides toward the northeast. Our observation that the persistent northeastern indentation of India powers the evolution of eastern Tibetan river systems is in agreement with the numerical models with lateral advection[45].

The current macroscopic configuration of the eastern Tibetan river systems seems to be the fluvial expression of tectonic deformations. England and Houseman[48] proposed that much of the post-Eocene convergence between India and Eurasia has been accommodated by the distributed crustal thickening (Fig. 4). The NE 21° component of crustal velocity controls the spatial patterns of crustal mass flux[38,46,47]. The northeastern descent of tectonic strain around the eastern Tibetan Plateau introduces directionally dependent regional topographic characteristics and builds up the widely distributed asymmetric dividing ranges with similar characteristic orientations. Dividing ranges rise and migrant, drainage networks develop toward an erosional balance with the distributed crustal thickening in the eastern Tibetan Plateau[25,28].

River system evolution in a tectonically active area with continual perturbations. Although the macroscopic configuration of eastern Tibetan river systems is controlled by tectonic drivers, as we zoom into smaller scales, low stream-order (1–5) drainage networks lose the signal of tectonics (Fig. 3). Indeed, the structures of low stream-order drainage networks in the eastern Tibetan Plateau display self-similarity features[26]. Progressive numerical simulations have prompted the maturity of optimal channel network models to elucidate the self-similarity structure of drainage system[36,49,50]. The optimal channel network models suggest that the fluvial self-organization produces self-similarity structures endowed with minimum energy expenditure[26,50]. Despite simulated progress, key hypotheses of optimal channel network models including exogenous perturbations remain to be poorly tested in natural conditions[50].

The self-similarity characteristics in low stream-order (1–5) drainage networks and the gradual divergences of the R_a and R_l with increasing stream-orders reinforce that eastern Tibetan river systems are in the state of local optimum (Fig. 3). The in-stream processes yield a progressive lowering of the energy dissipation of the river systems and is depending on the constraints imposed by the dynamical exogenous conditions[25,49,50]. Morphological characteristics of the low-level eastern Tibetan river systems are closely related to the establishment of accessible optimum in the self-organization of open dissipative systems[26]. The drainage networks are willing to accept myopic changes if their impacts are favorable in the short run[50]. During persistent exogenic perturbations, the river systems are settling in for dynamically accessible states of local optimum[49,50]. Given the continual tectonic perturbations, such as the persistent northeastward indentation of India, the phenomenon that endogenic self-organization of river system becomes trapped in exogenic conditions highlights the importance of the local optimization of optimal channel network models in tectonically active areas worldwide.

Methods

Morphological characteristics of dividing ranges. We use a series of MATLAB functions implemented in the TopoToolbox v2[23] to calculate and map the morphological characteristics of eastern Tibetan dividing ranges. The dividing ranges analyzed in our study are based on the 90 m resolution digital elevation model (DEM) from the Shuttle Radar Topography Mission. Gilbert metrics quantify across-divide topographic differences and thus are widely recognized as the determining factors in divide mobility[2,21,51]. Hillslope relief (HR) is the focus Gilbert metric of our study and is defined as the elevation difference between a point on the dividing range and the point in the stream to which it flows to[20]. We identify dividing ranges that have distinct across-divide differences in HR are asymmetric. The threshold for identifying asymmetric dividing ranges is a divide asymmetry index (DAI) > 0.02, and the DAI can be calculated as follows[20]

$$\mathrm{DAI} = \left| \frac{\triangle HR}{\sum HR} \right| \tag{1}$$

The divide segments at low divide distances have their courses along the DEM edge that are controlled by the truncated topography, and the drainage network due to their proximity to confluences. To avoid noise, the threshold of divide distance to >5 km is used to eliminate some unreal divides and minimize the influence of divides that are close to streams[20]. The vectors of divide asymmetry (Fig. 2) are established based on the orientations of the divide segments and their mean magnitudes of DAI.

Geometries of drainage networks. The extraction of eastern Tibetan drainage networks is carried out using the DEMRiver program developed by Bai et al.[52]. This program introduces a size-balanced binary search tree method to improve the computation efficiency, and it has advantages in the accuracy and completeness of the obtained drainage networks. The extracted drainage networks are validated against delineated drainage networks from the remote sensing imageries to assess the accuracy. To maximize extraction accuracy with computational efficiency, a drainage area threshold of 0.324 km^2 (40 grid cells) is used in our study to objectively extract drainage networks from the Shuttle Radar Topography Mission DEM (the area of one grid cell is approximately 0.0081 km^2).

The geometry of the drainage network can be described by the different stream-order rules defined by Horton[53], Strahler[54], and Shreve[55]. Our analyses of drainage networks are expressed as Horton ratios. After encoding all the stream segments in the drainage networks, the average area (A_i) and length (L_i) of rivers with each stream order can be obtained. For the drainage networks with the highest stream-order (N), the area ratio (R_a) and length ratio (R_l) are described as

$$A_i = A_{i-1} R_a^i, \mathrm{i} = 2, \dots N \tag{2}$$

$$L_i = L_{i-1} R_l^i, \mathrm{i} = 2, \dots N \tag{3}$$

Catchment erosion rates. To detect the dynamics of divide migration, we focus on the across-divide differences in the catchment erosion rates. OCTOPUS, a database of worldwide cosmogenic radionuclide measurements in fluvial sediment[29], is used in our study. The collected cosmogenic radionuclide data are recalculated using the CAIRN model to maintain consistency between erosion rates identified by different researchers. The uncertainties of erosion rate are estimated from both internal (nuclide concentration uncertainties from measurements) and external (shielding and production rate) sources using Gaussian propagation of uncertainty following Mudd et al.[56].

Annual precipitation rates. To explore whether the evolution of river systems is controlled by exogenic climatic drivers, we characterize the spatial distribution of mean annual precipitation rates throughout the eastern Tibetan Plateau with the WorldClim dataset[57], which has a 1×1 km^2 grid resolution (Supplementary Fig. 3). WorldClim version 2.1 contains climate data from 1970 to 2000, this 30-year period is transient compared to the timescale of river system evolution, we suppose that the spatial variation of modern precipitation should be representative of longer periods, even if the absolute values differ. Whereas the precipitation pattern has been continuously quantified in WorldClim, and only discontinuous distributions of divide asymmetry are available, statistic tests concerning the influence of precipitation on divide migrations might be impracticable.

Directional statistics. We test whether the mean direction of asymmetries along the high-level divide is equal to the direction of the persistent squeeze between the India and Eurasia plates (NE 21°). The statistics is implemented in the Circular Statistics Toolbox for the MATLAB programming environment[58]. The null hypothesis (H_0) and alternative hypothesis (H_A) are as follows

H_0: The mean direction of asymmetries along the high-level divide is equal to NE 21°.

H_A: The mean direction of asymmetries along the high-level divide is not equal to NE 21°.

For our direction dataset, the h-value is 0, we thus cannot reject the null hypothesis that means the direction of asymmetries is equal to NE 21°. Indeed, the

direction of NE 21° is located within the upper and lower 95% confidence limits on the population mean ([340.14°, 26.64°], Fig. 4). We conclude that the direction of the persistent indentation of India coincides with the main orientations of high-level divide migration.

Data availability

The data that support the findings of this study are openly available in figshare at https://doi.org/10.6084/m9.figshare.13625264.

Code availability

This manuscript includes no code.

References

1. Willett, S. D., McCoy, S. W. & Beeson, H. W. Transience of the North American High Plains landscape and its impact on surface water. *Nature* **561**, 528 (2018).
2. Whipple, K. X., Forte, A. M., DiBiase, R. A., Gasparini, N. M. & Ouimet, W. B. Timescales of landscape response to divide migration and drainage capture: implications for the role of divide mobility in landscape evolution. *J. Geophys. Res.* **122**, 248–273 (2017).
3. Willett, S. D., McCoy, S. W., Perron, J. T., Goren, L. & Chen, C. Y. Dynamic reorganization of river basins. *Science* **343**, 1117 (2014).
4. Fan, N. N. et al. Abrupt drainage basin reorganization following a Pleistocene river capture. *Nat. Commun.* https://doi.org/10.1038/s41467-018-06238-6 (2018).
5. Yang, R., Willett, S. D. & Goren, L. In situ low-relief landscape formation as a result of river network disruption. *Nature* **520**, 526 (2015).
6. Dahlquist, M. P., West, A. J. & Li, G. Landslide-driven drainage divide migration. *Geology* **46**, 403–406 (2018).
7. Schwanghart, W. & Scherler, D. Divide mobility controls knickpoint migration on the Roan Plateau (Colorado, USA). *Geology* **48**, 698–702 (2020).
8. Molnar, P., England, P. & Martinod, J. Mantle dynamics, uplift of the Tibetan Plateau, and the Indian Monsoon. *Rev. Geophys.* **31**, 357–396 (1993).
9. Brookfield, M. E. The evolution of the great river systems of southern Asia during the Cenozoic India-Asia collision: rivers draining southwards. *Geomorphology* **22**, 285–312 (1998).
10. Clark, M. K. et al. Surface uplift, tectonics, and erosion of eastern Tibet from large-scale drainage patterns. *Tectonics* https://doi.org/10.1029/2002tc001402 (2004).
11. Chen, Y. et al. Detrital zircon U-Pb geochronological and sedimentological study of the Simao Basin, Yunnan: implications for the Early Cenozoic evolution of the Red River. *Earth Planet. Sci. Lett.* **476**, 22–33 (2017).
12. Clift, P. D. et al. A late eocene-oligocene through-flowing river between the upper Yangtze and South China Sea. *Geochem. Geophys. Geosyst.* https://doi.org/10.1029/2020GC009046 (2020).
13. Nie, J. S. et al. Rapid incision of the Mekong River in the middle Miocene linked to monsoonal precipitation. *Nat. Geosci.* **11**, 944 (2018).
14. Burbank, D. W. et al. Decoupling of erosion and precipitation in the Himalayas. *Nature* **426**, 652–655 (2003).
15. Zeitler, P. K. et al. Erosion, Himalayan geodynamics, and the geomorphology of metamorphism. *GSA Today* **11**, 4–9 (2001).
16. Korup, O. & Montgomery, D. R. Tibetan plateau river incision inhibited by glacial stabilization of the Tsangpo gorge. *Nature* **455**, 786–U784 (2008).
17. Wang, P. et al. Tectonic control of Yarlung Tsangpo Gorge revealed by a buried canyon in Southern Tibet. *Science* **346**, 978–981 (2014).
18. Zhang, H. P. et al. Pleistocene drainage reorganization driven by the isostatic response to deep incision into the northeastern Tibetan Plateau. *Geology* **42**, 303–306 (2014).
19. Hallet, B. & Molnar, P. Distorted drainage basins as markers of crustal strain east of the Himalaya. *J. Geophys. Res.* **106**, 13697–13709 (2001).
20. Scherler, D. & Schwanghart, W. Drainage divide networks—Part 1: identification and ordering in digital elevation models. *Earth Surf. Dyn.* **8**, 245–259 (2020).
21. Forte, A. M. & Whipple, K. X. Criteria and tools for determining drainage divide stability. *Earth Planet. Sci. Lett.* **493**, 102–117 (2018).
22. Burbank, D. W. et al. Bedrock incision, rock uplift and threshold hillslopes in the northwestern Himalayas. *Nature* **379**, 505–510 (1996).
23. Schwanghart, W. & Scherler, D. Short Communication: TopoToolbox 2-MATLAB-based software for topographic analysis and modeling in Earth surface sciences. *Earth Surf. Dyn.* **2**, 1–7 (2014).

24. Schmidt, J. L. et al. Knickpoint evolution on the Yarlung river: evidence for late Cenozoic uplift of the southeastern Tibetan plateau margin. *Earth Planet. Sci. Lett.* **430**, 448–457 (2015).

25. Allen, P. A. Time scales of tectonic landscapes and their sediment routing systems. *Geol. Soc. Spec. Publ.* **296**, 7–28 (2008).

26. Dodds, P. S. & Rothman, D. H. Scaling, universality, and geomorphology. *Annu. Rev. Earth Planet. Sci.* **28**, 571–610 (2000).

27. Bierman, P. R. Rock to sediment—slope to sea with Be-10—rates of landscape change. *Annu. Rev. Earth Planet. Sci.* **32**, 215–255 (2004).

28. Perron, J. T., Richardson, P. W., Ferrier, K. L. & Lapotre, M. The root of branching river networks. *Nature* **492**, 100 (2012).

29. Codilean, A. T. et al. OCTOPUS: an open cosmogenic isotope and luminescence database. *Earth Syst Sci. Data* **10**, 2123–2139 (2018).

30. Finnegan, N. J. et al. Coupling of rock uplift and river incision in the Namche Barwa-Gyala Peri massif, Tibet. *Geol. Soc. Am. Bull.* **120**, 142–155 (2008).

31. King, G. E., Herman, F. & Guralnik, B. Northward migration of the eastern Himalayan syntaxis revealed by OSL thermochronometry. *Science* **353**, 800–804 (2016).

32. Henck, A. C., Huntington, K. W., Stone, J. O., Montgomery, D. R. & Hallet, B. Spatial controls on erosion in the Three Rivers Region, southeastern Tibet and southwestern China. *Earth Planet. Sci. Lett.* **303**, 71–83 (2011).

33. Ansberque, C. et al. Denudation pattern across the Longriba fault system and implications for the geomorphological evolution of the eastern Tibetan margin. *Geomorphology* **246**, 542–557 (2015).

34. Harkins, N., Kirby, E., Heimsath, A., Robinson, R. & Reiser, U. Transient fluvial incision in the headwaters of the Yellow River, northeastern Tibet, China. *J. Geophys. Res.* https://doi.org/10.1029/2006jf000570 (2007).

35. Ouimet, W. B., Whipple, K. X. & Granger, D. E. Beyond threshold hillslopes: channel adjustment to base-level fall in tectonically active mountain ranges. *Geology* **37**, 579–582 (2009).

36. Rodríguez-Iturbe, I. & Rinaldo, A. *Fractal River Basins: Chance and Self-organization.* (Cambridge University Press, 1997).

37. Godard, V. et al. Dominance of tectonics over climate in Himalayan denudation. *Geology* **42**, 243–246 (2014).

38. Wang, Q. et al. Present-day crustal deformation in China constrained by global positioning system measurements. *Science* **294**, 574–577 (2001).

39. Molnar, P. & Stock, J. M. Slowing of India's convergence with Eurasia since 20 Ma and its implications for Tibetan mantle dynamics. *Tectonics* https://doi.org/10.1029/2008tc002271 (2009).

40. Zhao, J. M. et al. The boundary between the Indian and Asian tectonic plates below Tibet. *Proc. Natl Acad. Sci. USA* **107**, 11229–11233 (2010).

41. Zhang, P. Z. et al. Continuous deformation of the Tibetan Plateau from global positioning system data. *Geology* **32**, 809–812 (2004).

42. Willett, S. D., Slingerland, R. & Hovius, N. Uplift, shortening, and steady-state topography in active mountain belts. *Am. J. Sci.* **301**, 455–485 (2001).

43. Miller, S. R., Slingerland, R. L. & Kirby, E. Characteristics of steady state fluvial topography above fault-bend folds. *J. Geophys. Res.* https://doi.org/10.1029/2007jf000772 (2007).

44. Goren, L., Willett, S. D., Herman, F. & Braun, J. Coupled numerical-analytical approach to landscape evolution modeling. *Earth Surf. Processes Landf.* **39**, 522–545 (2014).

45. He, C. Q. et al. Constraining tectonic uplift and advection from the main drainage divide of a mountain belt. *Nat. Commun.* https://doi.org/10.1038/s41467-020-20748-2 (2021).

46. Zheng, G. et al. Crustal deformation in the India-Eurasia collision zone from 25 years of GPS measurements. *J. Geophys. Res.* **122**, 9290–9312 (2017).

47. Wang, M. & Shen, Z. K. Present-day crustal deformation of continental China derived from GPS and its tectonic implications. *J. Geophys. Res.* https://doi.org/10.1029/2019jb018774 (2020).

48. England, P. & Houseman, G. Finite strain calculations of continental deformation .2. Comparison with the India-Asia collision zone. *J. Geophys. Res.* **91**, 3664–3676 (1986).

49. Maritan, A., Colaiori, F., Flammini, A., Cieplak, M. & Banavar, J. R. Universality classes of optimal channel networks. *Science* **272**, 984–986 (1996).

50. Rinaldo, A., Rigon, R., Banavar, J. R., Maritan, A. & Rodriguez-Iturbe, I. Evolution and selection of river networks: statics, dynamics, and complexity. *Proc. Natl Acad. Sci. USA* **111**, 2417–2424 (2014).

51. Gilbert, G. K. *Geology of the Henry Mountains.* (Washington, D.C., 1877).

52. Bai, R., Li, T. J., Huang, Y. F., Li, J. Y. & Wang, G. Q. An efficient and comprehensive method for drainage network extraction from DEM with billions of pixels using a size-balanced binary search tree. *Geomorphology* **238**, 56–67 (2015).

53. Horton, R. E. Erosional development of streams and their drainage basins—hydrophysical approach to quantitative morphology. *Geol. Soc. Am. Bull.* **56**, 275–370 (1945).

54. Strahler, A. N. Quantitative analysis of watershed geomorphology. *Eos Trans. Am. Geophys. Union* **38**, 913–920 (1957).

55. Shreve, R. L. Statistical law of stream numbers. *J. Geol.* **74**, 17 (1966).

56. Mudd, S. M., Harel, M. A., Hurst, M. D., Grieve, S. W. D. & Marrero, S. M. The CAIRN method: automated, reproducible calculation of catchment-averaged denudation rates from cosmogenic nuclide concentrations. *Earth Surf Dyn.* **4**, 655–674 (2016).

57. Fick, S. E. & Hijmans, R. J. WorldClim 2: new 1-km spatial resolution climate surfaces for global land areas. *Int. J. Climatol.* **37**, 4302–4315 (2017).

58. Berens, P. CircStat: a MATLAB toolbox for circular statistics. *J. Stat. Softw.* **31**, 1–21 (2009).

Acknowledgements

Author contributions

Y.C. and B.W. conceived the study. Y.C., Z.X. and J.Z. performed the computations. B.Z., R.Z., Y.X., M.L. and B.L. conducted the morphological interpretations. Y.C., B.W., Z.X. and J.Z. constructed the conceptive model. All authors contributed to the writing.

Competing interests

The authors declare no competing interests.

Additional information

Supplementary information The online version contains supplementary material available at https://doi.org/10.1038/s43247-021-00330-4.

Correspondence and requests for materials should be addressed to Baosheng Wu.

Peer review information *Communications Earth & Environment* thanks Niannian Fan and the other, anonymous, reviewer(s) for their contribution to the peer review of this work. Primary Handling Editors: Joe Aslin, Heike Langenberg.

Reprints and permission information is available at http://www.nature.com/reprints

Publisher's note Springer Nature remains neutral with regard to jurisdictional claims in published maps and institutional affiliations.